

A Study of Aqueous Solutions by Nuclear Magnetic Resonance

By Edmund R. Malinowski, Stevens Institute of Technology, Castle Point Station, Hoboken, New Jersey, for Office of Saline Water, J. A. Hunter, Director; W. Sherman Gillam, Assistant Director, Research; W. H. McCoy, Chief, Chemical Physics Division

Grant No. 14-01-0001-377

UNITED STATES DEPARTMENT OF THE INTERIOR • Stewart L. Udall, Secretary
Max N. Edwards, Assistant Secretary for Water Pollution Control

Created in 1849, the Department of the Interior—America's Department of Natural Resources—is concerned with the management, conservation, and development of the Nation's water, wildlife, mineral, forest, and park recreational resources. It also has major responsibilities for Indian and Territorial affairs.

As the Nation's principal conservation agency, the Department of the Interior works to assure that nonrenewable resources are developed and used wisely, that park and recreational resources are conserved for the future, and that renewable resources make their full contribution to the progress, prosperity, and security of the United States—now and in the future.

FOREWORD

This is one of a continuing series of reports designed to present accounts of progress in saline water conversion and the economics of its application. Such data are expected to contribute to the long-range development of economical processes applicable to low-cost demineralization of sea and other saline water.

Except for minor editing, the data herein are as contained in a report submitted by the contractor. The data and conclusions given in the report are essentially those of the contractor and are not necessarily endorsed by the Department of the Interior.

FINAL REPORT

A STUDY OF AQUEOUS SOLUTIONS BY
NUCLEAR MAGNETIC RESONANCE

by

Dr. Edmund R. Malinowski
Principal Investigator

Stevens Institute of Technology
Hoboken, New Jersey

November 10, 1967

Office of Saline Water, U. S. Department of the Interior
Grant No. 14-01-001-377

TABLE OF CONTENTS

	<u>Page</u>
Statement of the Problem	viii
Abstract	ix
Bulk-Magnetic-Susceptibilities Determined from NMR Spinning Side Bands using Coaxial Cells	1
Reference Standard for Studies Involving Temperature Dependence of ^{19}F Chemical Shifts	4
Preparation of Aqueous Solutions	8
Reference Standards	8
Preparation of Sample Cells for NMR Measurements	9
Modification of the NMR Spectrometer	9
Bulk-Magnetic-Susceptibility Correction Factors	10
Results and Treatment of Data	14
Discussion	22
Labile Equilibrium	22
Motivations for This Investigation	24
Trends of the Data	25
Curve Fitting	30
The Physical Model	33
A. Short-Range Order Theory	35
B. Phase Diagram	35
C. Chemical Shift Data	35
Mathematical Development	36
Correlation of Theory with Experiment	42
Range of Validity of the Dilute Approximation	44
Verification of the Theory	44
A. Partial Molar Heat Content	45
B. Potassium Resonance Data	47
Conclusions	50

TABLE OF CONTENTS
(Continued)

	<u>Page</u>
Suggestions for Future Work	51
References	52
Research Personnel	54
Degrees Attained or Expected	54
List of Publications	54
Papers to be Submitted for Publication	54

LIST OF TABLES

<u>Table No.</u>		<u>Page</u>
I	Chemical Shifts of p-Difluorobenzene as a Function of Temperature	7
II	Observed F^{19} Shifts and Spinning Sideband Bulk- Susceptibility Factors for Reference Standards as a Function of Temperature	17
III	Observed F^{19} Shifts and Nonspinning Peak Separations as a Function of T for KF Solutions	18
IV	Observed F^{19} Shifts and Nonspinning Peak Separations as a Function of Temperature for RbF Solutions	19
V	Observed F^{19} Shifts and Nonspinning Peak Separations at 25°C and 50°C for CsF Solutions	20
VI	Table of Chemical Shifts and Bulk Susceptibilities for Aqueous Alkali Metal Fluoride Solutions	21
VII	Values of the Mean Unbiased Error, S , Tabulated in PPM	32
VIII	Coefficients of Equation (15)	33
IX	The Parameters of the Labile Equilibrium Theory as Calculated with Eqs. 35-39	43
X	Comparison of Calculated Changes in the Partial Molar Heat Content of KF at 25°C with those given by Harned and Owen ²⁶	48

LIST OF FIGURES

<u>Figure No.</u>		<u>Page</u>
1	Proportional Controller for Varian Variable Temperature NMR Probe	11
2	F^{19} Shifts (Relative to p-Difluorobenzene at 0°C) of Aqueous RbF Solutions as a Function of Molality at Different Temperatures	26
3	F^{19} Shift (Relative to p-Difluorobenzene at 0°C) of Aqueous RbF Solutions as a Function of Temperature at Different Molalities	27
4	F^{19} Shift (Relative to p-Difluorobenzene at 0°C) of Aqueous KF Solutions as a Function of Molality at Different Temperatures	28
5	F^{19} Shifts (Relative to p-Difluorobenzene at 0°C) of Aqueous KF, RbF and CsF Solutions as a Function of Molality at 50°C	29
6	Natural Logarithm of the Equilibrium Constant, K_D , as a Function of $1/T$.	46

STATEMENT OF THE PROBLEM

The treatment and purification of water poses a difficult and serious problem. In order to solve such problems, a knowledge of the ionic and intermolecular forces at play in aqueous solutions is of fundamental importance. The present study focuses attention on the nuclear magnetic resonance of the fluoride ion in aqueous solutions. The F^{19} chemical shifts of KF, RbF and CsF are measured as a function of temperature and concentration. It was initially surmised that such a study would lead to a better understanding of (1) the nature of ionic hydrates and (2) the equilibrium between the water and the ionic hydrates.

ABSTRACT

This investigation is a study of the natural forces between water molecules and ions by the technique of nuclear magnetic resonance (NMR). The fluoride ion was chosen as the object of study because it produces an accurate NMR spectrum. Effects of temperature and concentration on the F^{19} chemical shift of aqueous solutions of KF, RbF and CsF are measured.

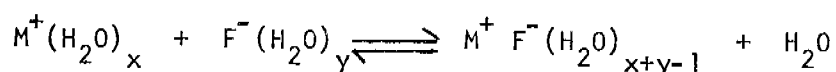
In the course of this work a new and accurate technique for making bulk-susceptibility corrections was developed. The technique involves the use of coaxial sample cells. The area and frequency of the side bands which result when the coaxial cells are rotated in the magnetic field are found to be related to the bulk susceptibilities of the sample and external standard. This technique is of general interest to anyone requiring bulk-susceptibility data. Details of this work have been published in the Journal of Chemical Physics, 45, 4355 (1966).

Because F^{19} shifts are strongly dependent on temperature, special techniques for referencing the shifts were developed. A method of temperature calibration, based on heteronuclear double resonance, was successfully developed. This method consists of irradiating the F^{19} nuclei of paradifluorobenzene while observing the H^1 resonance. From such experiments the F^{19} shifts are referenced with respect to the H^1 resonance of gaseous ethane which does not vary with temperature. This work has been published in the Journal of Chemical Physics, 47, 1560 (1967).

Plots of F^{19} shifts versus molality, at a given temperature, for

the various salts (KF, RbF and CsF) converge to a common point at infinite dilution. This clearly indicates that the fluoride ion behaves independently from the cation at infinite dilution. The common intercept varies with temperature, moving to higher field with increasing temperature. This sensitivity to temperature could be the result of either the hydrated fluoride ion being promoted to a higher vibrational energy level or the breakdown of hydrogen bonds of water in the secondary layer, or, possibly, a combination of both of these effects.

At concentrations below four molal all salts exhibit a non-linear decrease in F^{19} chemical shift with increasing molality. The non-linearity is explained on the basis of the formation of aquo-ion pairs, according to the equilibrium:



From the shift data, equilibrium constants are calculated, from which ΔH of the reaction is obtained. The resulting ΔH is shown to be in general agreement with partial molar heat contents derived from heats of dilution measurements.

Bulk Magnetic Susceptibilities Determined from
NMR Spinning Side Bands using Coaxial Cells

In high resolution NMR spectra prominent spinning side bands are observed for the material in the annular region of a coaxial sample cell. It is generally believed that these side bands arise because of imperfections in the glass cells and inhomogeneity of the applied magnetic field. We contend that the observed side bands are a property of the geometry of the coaxial system. Side bands would still be observed even if the coaxial cells were free from all imperfections and the applied magnetic field were homogeneous. We would also like to point out that this phenomenon can be used to test the field-modulation theory developed by Williams and Gutowsky.¹ Preliminary measurements clearly indicate that the correct interpretation may be used to determine the bulk susceptibility of liquids and gases.

The magnetic field H_a in the annular region for a coaxial cell is a function of the applied field, H_0 ; the volume magnetic susceptibilities of the material in the central tube, the material in the annular region, the glass and the surrounding air, χ_c , χ_a , χ_g and χ_{air} , respectively; the inner and outer radii of the inner glass tube, a and b , respectively; and the polar coordinates r and θ ($\theta = 0$ is the direction of the applied field). Namely,^{2,3}

$$H_a = \langle H_a \rangle + \Delta H_a \cos 2\theta \quad (1)$$

where $\langle H_a \rangle \equiv [1 - 2\pi(\chi_a - \chi_{air})] H_0$ and $\Delta H_a \equiv [a^2(\chi_c - \chi_g) + b^2(\chi_g - \chi_a)] 2\pi H_0 / r^2$.

Zimmerman and Foster² argue that a molecule in the annular region of a spinning coaxial system experiences an effective field $\langle H_a \rangle$. This is equivalent to averaging equation (1) over θ .

In the coaxial system the effect of spinning causes the individual molecules in the annular region to experience an oscillatory field as described by equation (1). An oscillatory field produces side bands¹ at $\nu_0 \pm n\nu_m$, where ν_0 is the fundamental resonance, ν_m is the frequency of the oscillatory field and n is 1, 2, Since H_a is periodic in π , the separation between two adjacent side bands should be $\nu_m = 2\nu_s$, where ν_s is the spinning frequency. In our laboratory this has been observed. The sample spinning frequency was measured with a General Radio Strobotac driven by a Hewlett-Packard 200 CDR wide-range oscillator. The driving frequency was counted within ± 0.1 cps with a Hewlett-Packard 523 DR Electronic Counter. The side-band separation for various substances was recorded with a Varian Associate A60A spectrometer operating at 60 Mc/sec. In each case the separation between neighboring side bands was twice the spinner frequency as predicted.

Equation (1) indicates that the magnitude of the field variation depends upon the magnetic susceptibilities of the substances involved. If the annular region is sufficiently narrow an average value of r may be used and the William-Gutowsky theory¹ for field modulation can be applied directly. According to this theory the intensity I_n of the n -th order side band is directly proportional to $J_n^2(k)$, where J_n is the n -th order Bessel function of the first kind and the argument $k = \gamma H / 2\pi\nu_m$. H is the maximum amplitude and ν_m the frequency of the field modulation. For the field described by equation (1)

$$k = \frac{\gamma \Delta H_a}{4\pi\nu_s} \quad (2)$$

This argument indicates that side-band intensities can be used to determine a unique value of k for a given spinning frequency. Equation (2) can then be used to calculate ΔH_a , from which bulk susceptibilities can be obtained.

Many different techniques can be used to obtain k . One simple method, for example, is to adjust the spinner frequency so that the intensity of the fundamental band exactly equals the intensity of the first side band, i.e. $I_0 = I_1$ and thus $J_0^2(k) = J_1^2(k)$. An examination of tables of Bessel functions reveals several values of k which obey this equation. From these values the correct value of k is chosen by considering the relative intensities of the higher-order side bands. We have studied two systems at 42°C, each with 1,2-dibromoethane in the annular region. The central tube contained acetone in system (1) and carbon tetrachloride in system (2). Under the conditions described above, we found $k = 1.4347$ from tables of Bessel functions. The spinning frequencies of the coaxial cells had to be adjusted to 36.9 cps and 20.5 cps for systems (1) and (2), respectively. From the data and equation (2), we obtained values for ΔH_a . To test this method we calculated the bulk susceptibility of the glass cells by applying the defining equation for ΔH_a and known values for the dimensions of the coaxial system⁴ and bulk susceptibilities of the substances employed. We found the bulk susceptibility of the glass to be -0.817×10^{-6} emu and -0.818×10^{-6} emu for systems (1) and (2) respectively. This agreement verifies the interpretation. One could obtain the bulk susceptibilities of liquids and gases after such calibration of the cells. This work has been published in the Journal of Chemical Physics.⁵

This technique has been used for determining the temperature dependence of ^{19}F shifts as described in the following section.

Reference Standard for Studies Involving
Temperature Dependence of ^{19}F Chemical Shifts

The most desirable reference standard for measuring ^{19}F chemical shifts as a function of temperature should have the following properties: (a) the reference should have a sharp signal, (b) the position of the reference signal should be independent of temperature and (c) the reference compound must be a liquid over the temperature range, 0 to 100°C. Unfortunately, no compound having all three properties was found. For this reason the requirement of a reference signal which is independent of temperature was relaxed and the sharp triplet of 1,2-dichlorohexafluoro-1-cyclopentene and, in some cases, the singlet of hexafluorobenzene were used as external references.

Studies involving ^{19}F chemical shifts as a function of temperature are subject to uncertainty if the temperature variation of the reference signal has not been established. To date, investigators⁶ using ^{19}F resonance have recognized, but have not accounted for such possible variations. We have developed a heteronuclear double resonance technique for measuring the "temperature-dependent shift" of the ^{19}F quintet of p-difluorobenzene. The temperature-dependent shift of other standards, such as hexafluorobenzene, can easily be determined from this information when used in conjunction with conventional external standard chemical shifts.

Our method is based upon the measurements and calculations of Petrakis and Sederholm.⁷ These workers have shown that the proton shift of gaseous ethane does not vary with temperature in the region from 25 to 100°C. Similar calculations performed in our laboratory indicate that gaseous fluorine compounds may exhibit sizable temperature-dependent shifts and therefore fluorine gases are not reliable standards. Our method requires

two experimental steps: (1) the chemical shift of the proton triplet of p-difluorobenzene relative to gaseous ethane is determined using coaxial sample cells; and (2) the signal separation between the proton triplet and the fluorine quintet of p-difluorobenzene is measured by heteronuclear double resonance. This information allows us to calculate the temperature-dependent shift of the fluorine quintet.

For p-difluorobenzene the fluorine temperature-dependent shift is related to the proton temperature-dependent shift by the equation⁸

$$\delta_F^O(T) = 1 - (\nu_T/f_T) (f_O/\nu_O) [1 - \delta_H^O(T)]. \quad (3)$$

In this expression $\delta_H^O(T) = \delta_H(T) - \delta_H(0)$, where $\delta_H(T)$ and $\delta_H(0)$ are the proton shifts measured relative to gaseous ethane at temperature T and 0°C, respectively. In other words, $\delta_H^O(T)$ is the proton shift at temperature T relative to that at 0°C. Similarly, δ_F^O is the fluorine shift at temperature T relative to the fluorine signal at 0°C. Also, ν_T and f_T are the fluorine and proton irradiating frequencies, respectively, necessary to resonate the proton and fluorine nuclei simultaneously at a given magnetic field strength, at temperature T. Since the H^1 and F^{19} nuclei of p-difluorobenzene are magnetically coupled these frequencies are measurable by heteronuclear double resonance. Our procedure for the decoupling experiment was the same as that of Paul and Grant⁸ with one exception. The magnitude of the proton irradiating frequency was kept below that necessary for complete decoupling of the fluorine quintet. This modified procedure allows us to determine the exact decoupling frequency by inspection of the asymmetry of the perturbed fluorine pattern.⁹

C. P. grade ethane (The Matheson Co.) at approximately 8 atm pressure

was sealed in the central tube of a Wilmad coaxial cell system.⁴ The annular region was filled with p-difluorobenzene, supplied by the Pierce Chemical Co. The F^{19} and H^1 shifts were measured with Varian DP-60 and A60A spectrometers operating at 56.4 mc/s and 60 mc/s, respectively. Bulk magnetic susceptibilities were determined using the spinning side-band technique,⁵ and the shifts were corrected for bulk susceptibility differences. The corrected shifts, $\delta_H^0(T)$, are shown in column 2 of Table I. The second irradiating frequency for the double resonance experiment was generated by an NMR Specialties SD60 Heteronuclear Spin Decoupler equipped with frequency lock. All frequencies were counted with a Hewlett-Packard 5245L Electronic Counter. The ratios f_T/v_T are listed in column 3 of Table I. The fourth column contains the values of $\delta_F^0(T)$ calculated from the equation above.

The determination of the temperature-dependent shifts provides experimentalists with the opportunity to conduct meaningful F^{19} studies that involve variable temperatures. The technique described here is applicable in general to other nuclei that exhibit coupling with protons.

We are greatly indebted to the Bell Telephone Laboratories, Inc., for the use of their heteronuclear decoupling apparatus, and to Ernest Anderson for valuable assistance in performing the decoupling experiments.

TABLE 1: CHEMICAL SHIFTS OF p-DIFLUOROBENZENE AS A FUNCTION OF TEMPERATURE

Temperature ($^{\circ}\text{C}$)	$\delta_{\text{H}}^{\text{O}}(\text{T})$ (ppm)	$f_{\text{T}}/\nu_{\text{T}}$	$\delta_{\text{F}}^{\text{O}}(\text{T})$ (ppm)
- 5	+ 0.021	1.063006384	+ 0.001
0	0.000	1.063006407	0.000
10	- 0.032	1.063006454	+ 0.013
25	- 0.066	1.063006525	+ 0.046
40	- 0.091	1.063006596	+ 0.087
55	- 0.112	1.063006666	+ 0.132
70	- 0.131	1.063006737	+ 0.180
85	- 0.143	1.063006808	+ 0.235
100	- 0.142	1.063006878	+ 0.302
Error on each Entry	\pm .013	$\pm 1.5 \times 10^{-8}$	± 0.020

Preparation of Aqueous Solutions

Preparation of aqueous solutions of KF having a concentration accuracy of $\pm 0.1\%$ is quite difficult since KF is extremely hygroscopic. We investigated several preparative techniques and adopted the one based on density data, as described below.

A nearly saturated solution of anhydrous KF (Baker & Adamson, Reagent Grade) was prepared using distilled, deionized water. After the entire batch was filtered to remove insoluble residue, an aliquot was diluted to a concentration falling within the range of density versus concentration data reported in the International Critical Tables. The density of the diluted aliquot was measured and the concentration of the stock solution was determined by calculation.

Accurate density versus concentration data is not available for RbF and CsF, therefore, stock solutions were prepared by weight. Fortunately RbF and CsF are not greatly hygroscopic. A vacuum dried, weighed amount of salt (K and K Laboratories, 99.9% pure) was added to a sufficient quantity of distilled deionized water in a preweighed flask to give a nearly saturated solution. The solution was then filtered through a preweighed filter and filter paper (Coors 27H, Millipore $1.2\ \mu$) to remove insoluble residue. The empty flask and filtering apparatus were vacuum dried and weighed and the weight of salt corrected for the amounts of residue.

For chemical shift measurements dilutions of the KF, RbF, and CsF stock solutions were prepared by weight.

Reference Standards

Hexafluorobenzene, p-difluorobenzene (both from the Pierce Organic Chemical Co.) and 1,2 dichlorohexafluorocyclopentene-1 (Columbia Organic Chemical Co.) were used as reference standards during different stages of

this investigation. These compounds exhibited no detectable impurities in the NMR spectra, and gas chromatography indicated that any impurity was much less than 0.1%.

Preparation of Sample Cells for NMR Measurements

To eliminate spurious results caused by the use of internal standards, external standards were used in conjunction with coaxial sample cell systems.⁴ A very small amount of reference standard was permanently sealed in the annular portion of a coaxial system by fusing the glass cells. With the reference compound sealed in the annular region several advantages accrue:

1. The usable temperature range of the reference compound is increased by at least 20°C (both hexafluorobenzene and 1,2-dichlorohexafluorocyclopentene-1 boil below 100°C).
2. The inner cell is easily cleaned and filled using a syringe and a long Teflon needle. One need not fear contaminating the standard.

Modifications of the NMR Spectrometer

In order to study the cation effect on the fluoride ion by nuclear resonance it is desirable to measure the F^{19} shifts of the alkali metal fluorides as a function of concentration over the entire solubility range. Survey measurements indicated a surprisingly wide range of chemical shifts for CsF solutions. To obtain accurate measurements we made improvements in the power supply, stabilizing loop and radio-frequency unit of the DP60 spectrometer. The autotransformer that controls the voltage applied to the magnet coils was replaced by a transformer with a higher current rating. Other improvements, such as replacing aged components, were also made. With

these modifications the field was made sufficiently stable. In order to measure F^{19} shifts of CsF solutions which scan a range of 25 ppm we decided to modify the radio-frequency generator according to the method of Alexakos and Cornwell.¹⁰ This modification allows chemical shifts over the range of 4 to 1300 ppm to be measured by the sideband technique. An added benefit is that the primary reference standard can be chosen from a large class of compounds. That is, the signal of the reference standard need not lie close to the fluoride ion resonance. In fact, to take advantage of the greatly increased signal-to-noise ratio of the calibration sideband we now use hexafluorobenzene as the primary standard instead of 1,2-dichlorohexafluorocyclopentene-1.

An SCR proportional temperature controller was built for the DP60 Spectrometer variable temperature probe.¹¹ With this unit we are able to maintain any desired temperature between -60°C and 150°C within $\pm 0.1^{\circ}\text{C}$. The circuit diagram is reproduced in Figure 1.

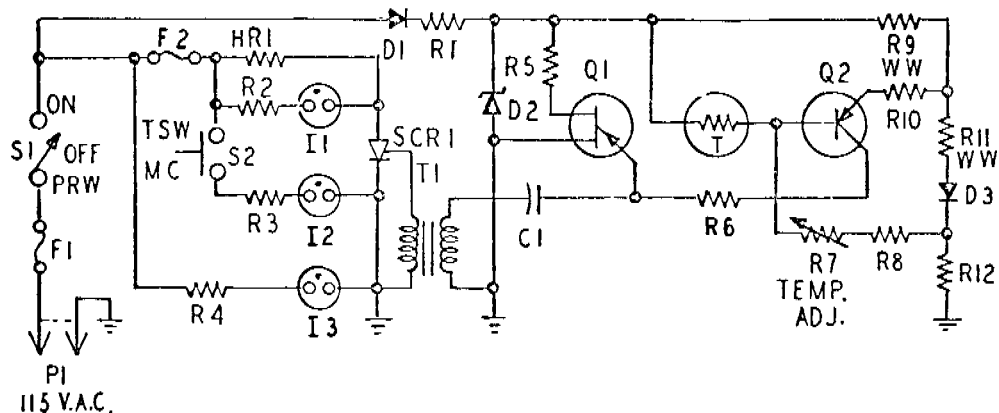
Bulk-Magnetic-Susceptibility Correction Factors

Since external reference standards were used in a concentric cylindrical sample cell system, it was necessary to apply a correction to the observed chemical shift due to the difference in bulk magnetic susceptibility of the sample and reference,¹² namely,

$$\delta_{\text{corrected}} = \delta_{\text{observed}} + \frac{2\pi}{3} (\chi_{V,\text{ref}} - \chi_{V,s}) \quad (4)$$

In this equation, $\chi_{V,\text{ref}}$ and $\chi_{V,s}$ are, respectively, the magnetic susceptibility per unit volume of the reference and the sample. (There is no correction necessary for concentric spherical sample tubes).

FIGURE 1. PROPORTIONAL CONTROLLER FOR VARIAN VARIABLE TEMPERATURE NMR PROBE



Symbol	Component	Symbol	Component
C1	0.25 μ f, 50V	R2	100K
D1	IN 2071	R3	200K
D2	IN 1353	R4	200K
D3	IN 2071	R5	470, 1W
F1	15A	R6	2.2K
F2	5A	R7	30K 10 TURN
HR1	4.5 Ω HEATER	R8	680
I1	NE2H	R9	300
I2	NE51	R10	270, 1W
I3	NE51	R11	300
Q1	2N491	R12	1K, 2W
Q2	IN 525	SCR1	2N685
R1	1.5K	T1	SPRAGUE 31Z382
T	THERMISTOR - LOCATED IN NMR PROBE INSERT		

Thermistor used should be chosen for minimum attainable temperature.

T_{min} ($^{\circ}$ C)	Resistance at 25 $^{\circ}$ C (Ω)	Fenwall Electronics Part #
-63	500	GD25J1
-17	5,000	GB35J1
10	15,000	GA42J1
51	100,000	GA51J1
95	500,000	GA55J1

To obtain the quantity $(\chi_{V,ref} - \chi_{V,s})$ without resorting to literature values, experimental techniques employing the NMR spectrometer were developed in this laboratory. A rigorous theoretical treatment outlined in a previous section forms the basis for these techniques. The spinning sideband technique previously described was used to obtain values of $\chi_{V,ref}$ and $\chi_{V,s}$ during the latter part of this investigation. Both the spinner design and spinner airflow system had to be modified to control the spinning frequency within ± 0.1 cps. The air flow rate was controlled using a cartesian diver pressure regulator (Manostat Corporation, Model #8).

The non-spinning cell technique^{2,3} was used to determine $(\chi_{V,ref} - \chi_{V,s})$ during the earlier phases of this work. The resonance signal of the reference in the annular region of a nonspinning coaxial cell system takes the shape of a camel hump. The frequencies of the low- and high-field humps, designated ν_{min} and ν_{max} , obey the following expression:

$$\Delta \equiv \frac{\nu_{max} - \nu_{min}}{\nu_0} = 4\pi \left| (\chi_s - \chi_g) \frac{a^2}{c^2} + (\chi_g - \chi_r) \frac{b^2}{c^2} \right| \quad (5)$$

Here χ_s , χ_g , and χ_r are the volume susceptibilities of the sample, glass, and reference, respectively; c is the inner radius of the outer glass tube; and a and b refer to the inner and outer radii of the inner glass tube.

If the sample region is evacuated, the resonance signal of the reference will again take the form of a camel hump. We may write

$$\Delta' \equiv \frac{\nu'_{max} - \nu'_{min}}{\nu_0} = 4\pi \left| (0 - \chi_g) \frac{a^2}{c^2} + (\chi_g - \chi_r) \frac{b^2}{c^2} \right| \quad (6)$$

Subtracting equations (6) from (5), we find

$$\Delta - \Delta' = 4\pi \frac{a^2}{c^2} \chi_s \quad (7)$$

Since the distances a and c are easily measurable, χ_s can be calculated uniquely after the sign of the quantity inside the magnitude symbols of equations (5) and (6) are determined by logical reasoning or from approximate literature values.

Results and Treatment of Data

In measuring the fluorine shifts of KF, RbF and CsF the sharp triplet of 1,2-dichlorohexafluoro-1-cyclopentene and, in some cases, the singlet of hexafluorobenzene were used as external references. Measurements were conducted over the temperature range from 0 to 100°C. Bulk-susceptibility corrections were made in part utilizing the spinning coaxial sample technique described previously and in part using the stationary sample technique. All shifts were then rereferenced to the signal of p-difluorobenzene at 0°C, the temperature shift of p-difluorobenzene having been determined by the heteronuclear spin decoupling technique described earlier (see Table I).

Experimental measurements were conducted in such a manner that the shifts of the fluoride ions of the aqueous solutions could be referenced with respect to p-difluorobenzene at 0°C. Since coaxial cells were employed, bulk-susceptibility corrections were required as stated by Eq. (4). In actual practice the following equation was used

$$\begin{aligned} \delta(F^T-PDB^0) &= \delta_{\text{obs}}(F^T-HFB^T) - \delta_{\text{obs}}(PDB^T-HFB^T) \\ &+ \delta(PDB^T-PDB^0) + \frac{2}{3}\pi [\chi(PDB^0) - \chi(F^T)] \end{aligned} \quad (8)$$

The term $\delta(F^T-PDB^0)$ is the F^{19} shift of the fluoride ion at temperature T relative to the fluorine signal of p-difluorobenzene (PDB) at 0°C. The term $\delta_{\text{obs}}(F^T-HFB^T)$ is the experimentally observed shift of the fluoride ion relative to hexafluorobenzene (HFB); the measurement being conducted at temperature T with hexafluorobenzene in the annular region. Similarly, $\delta_{\text{obs}}(PDB^T-HFB^T)$ is the observed shift of p-difluorobenzene relative to hexafluorobenzene; the measurement again being conducted at the same temperature T with hexafluorobenzene in the annular region. The term $\delta(PDB^T-PDB^0)$ is

the F^{19} temperature-dependent shift of p-difluorobenzene at temperature T relative to the signal at 0°C . Values for this term at different temperatures, determined by heteronuclear decoupling experiments are given in the fourth column of Table I. The last term on the right-hand side of Eq. (8) represents the bulk-susceptibility correction factors. The symbol $\chi(\text{PDB}^0)$ is the volume magnetic susceptibility of p-difluorobenzene measured at 0°C , whereas $\chi(F^T)$ is the volume magnetic susceptibility of the aqueous fluoride solution at temperature T .

Values for $\chi(\text{PDB}^0)$ and $\chi(F^T)$ were determined experimentally with the NMR spectrometer. As discussed previously, the signal of a sample in the annular region of a coaxial cell system takes the shape of a camel hump when the cell remains stationary in the magnetic field. The separation, Δ , between the low-field and high-field humps is related to the dimensions and bulk-susceptibilities of the cell system as shown in Eq. (5). To obtain $\chi(\text{PDB}^0)$ one simply places some standard, such as hexafluorobenzene, in the annular region and measures Δ when the inner cell is completely evacuated and again when the inner cell contains p-difluorobenzene. Of course both measurements must be carried out at 0°C . Eq. (5) applies to both of these experiments and upon writing such appropriate expressions one finds that χ_g and χ_f can be mathematically eliminated. Consequently, since $\chi_{\text{vacuum}} = 0$,

$$\chi(\text{PDB}^0) = \frac{c^2}{4\pi a^2} \left\{ \Delta(\text{PDB}^0\text{-HFB}^0) - \Delta(\text{vac}^0\text{-HFB}^0) \right\} \quad (9)$$

A much more accurate way of determining Δ is to study the "spinning side-bands" which result when the coaxial system is rotated. This method has been discussed previously. If the spinner frequency is adjusted so that the intensity of the fundamental band exactly equals the intensity of the

first side band then $\Delta = 2 k D = 2.8694D$, since $k = 1.4347$ for these conditions. D is the separation, in ppm, between the fundamental band and first side band. Using this technique we determined that

$$\Delta(\text{vac}^{\text{O}}\text{-HFBO}) = 4.108 \pm 0.014 \text{ ppm}$$

and
$$\Delta(\text{PDB}^{\text{O}}\text{-HFBO}) = -0.376 \pm 0.010 \text{ ppm.}$$

From the dimensions of the cells we found $c^2/4\pi a^2 = 0.14956$. Substituting these values into Eq. (9) we obtained

$$\chi(\text{PDB}^{\text{O}}) = -0.671 \pm 0.003 \text{ ppm.}$$

In order to determine $\chi(\text{F}^{\text{T}})$ we employed an expression analogous to Eq. (9), namely

$$\chi(\text{F}^{\text{T}}) = \frac{c^2}{4\pi a^2} \left\{ \Delta(\text{F}^{\text{T}}\text{-HFBT}) - \Delta(\text{vac}^{\text{T}}\text{-HFBT}) \right\} \quad (10)$$

At a constant temperature T the value of $\Delta(\text{F}^{\text{T}}\text{-HFBT})$ and the value of $\Delta(\text{vac}^{\text{T}}\text{-HFBT})$ were determined either by the nonspinning or spinning sideband techniques. The first term in the parentheses signifies the material in the central tube and the second indicates the material in the annular region.

In certain experiments 1,2-dichlorohexafluorocyclopentene-1 (CFC) was used as the external standard. Experimental values for δ and Δ for various measurements are presented in Tables II, III, IV and V. Upfield shifts are chosen to be positive, downfield negative.

Using the values given in Tables II through V and Eq. (8) the F^{19} shifts, corrected for bulk-susceptibility differences and referenced with respect to p-difluorobenzene at 0°C , were determined for a variety of aqueous solutions from 0 to 100°C . A compilation of these results is presented in Table VI.

TABLE II: OBSERVED F^{19} SHIFTS AND SPINNING SIDEBAND
 BULK-SUSCEPTIBILITY FACTORS FOR REFERENCE STANDARDS
 AS A FUNCTION OF TEMPERATURE

$T(^{\circ}C)$	δ_{obs} (ppm)			Δ (ppm)*	
	(PDB^T-HFB^T)	(PDB^T-CFC^T)	(PDB^T-PDB^O)	(vac^T-HFB^T)	(vac^T-CFC^T)
0	-46.130	5.492	0.000	4.108	4.464
10	-46.092	5.493	0.013	3.980	4.326
25	-46.035	5.500	0.046	3.786	4.112
40	-45.977	5.511	0.087	3.594	3.894
50	-45.938	5.518	0.115	3.460	3.754
55	-45.920	5.523	0.132	3.394	3.680
70	-45.863	5.537	0.180	3.202	3.462
85	-45.805	5.557	0.235	3.010	3.250
100	-45.747	5.588	0.302	2.814	3.032
	$\pm .007$	$\pm .006$	$\pm .020$	$\pm .016$	$\pm .040$

* Determined from spinning-sample coaxial-cell technique.

TABLE III: OBSERVED F^{19} SHIFTS AND NONSPINNING PEAK SEPARATIONS
AS A FUNCTION OF T FOR KF SOLUTIONS

Molal Conc.	--- $^*\delta_{\text{obs}}(F^T - \text{CFC}^T)$ in ppm ---				----- $^*\Delta(F^T - \text{CFC}^T)$ in ppm -----			
	<u>0°C</u>	<u>25°C</u>	<u>50°C</u>	<u>100°C</u>	<u>0°C</u>	<u>25°C</u>	<u>50°C</u>	<u>100°C</u>
.174	3.400	-	-	-	-.636	-	-	-
.530	3.253	3.843	4.543	6.059	-.641	-.969	-1.131	-1.775
1.245	2.985	3.674	4.417	5.990	-.748	-1.065	-1.236	-1.792
3.280	2.515	3.356	4.187	5.871	-.978	-1.241	-1.457	-1.936
5.44	2.344	3.291	4.225	6.079	-1.108	-1.396	-1.662	-2.221
8.00	2.615	3.422	4.342	6.224	-1.346	-1.574	-1.812	-2.348
11.47	3.178	-	-	6.735	-1.418	-	-	-2.617
14.37	4.029	4.802	5.707	7.305	-1.618	-1.843	-2.068	-2.573
	$\pm .008$	$\pm .017$	$\pm .010$	$\pm .025$	$\pm .030$	$\pm .025$	$\pm .040$	$\pm .118$

*All KF solutions were measured relative to CFC using stationary sample technique for bulk-susceptibility corrections.

TABLE IV: OBSERVED F^{19} SHIFTS AND NONSPINNING PEAK SEPARATIONS
AS A FUNCTION OF TEMPERATURE FOR RbF SOLUTIONS

Molal Conc.	--- (a) $\delta_{\text{obs}}(F^T - \text{HFB}^T)$ in ppm ---			--- (a) $\Delta_{\text{obs}}(F^T - \text{HFB}^T)$ in ppm ---		
	<u>0°C</u>	<u>25°C</u>	<u>50°C</u>	<u>0°C</u>	<u>25°C</u>	<u>50°C</u>
0.37	-	-47.804	-47.038	-	-1.219	-1.502
0.78	-48.769	-48.053	-	-.989	-1.313	-
1.10	-49.022	-48.254	-47.479	-1.049	-1.325	-1.686
1.69	-49.298	-48.450	-47.729	-1.111	-1.416	-1.701
2.21	-	-48.746	-	-	-1.479	-
2.78	-49.821	-48.986	-48.222	-1.269	-5.82	-1.853
4.10	-	-49.507	-48.764	-	-1.712	-1.973
4.40	-50.436	-	-	-1.462	-	-
4.72	-	-49.743	-	-	-1.798	-
5.38	-50.785	-49.974	-49.291	-1.563	-1.871	-1.978
6.12	-	-50.216	-	-	-1.935	-
6.52	-51.178	-	-49.698	-1.621	-	-2.061
6.91	-	-50.471	-	-	-2.013	-
7.50	-	-50.635 ^(b)	-50.001	-	-1.990 ^(b)	-2.146
8.48	-51.740	-50.944	-50.340	-1.745	-2.133	-2.196
9.96	-	-51.389	-50.814	-	-2.211	-2.331
11.72	-52.647	-51.904	-51.368	-2.048	-2.326	-2.452
14.38	-53.377	-52.714	-52.197	-2.114	-2.424	-2.582
	$\pm .010$	$\pm .008$	$\pm .008$	$\pm .042$	$\pm .030$	$\pm .027$

(a) All RbF solutions were measured relative to HFB. Bulk susceptibility splittings by stationary sample technique.

(b) The 7.5 M solution was measured also relative to CFC:
 $\delta(F^{50} - \text{CFC}^{50}) = +0.898$ ppm, $\Delta(F^{50} - \text{CFC}^{50}) = -1.465$ ppm.

TABLE V: OBSERVED F^{19} SHIFTS AND NONSPINNING PEAK SEPARATIONS
AT 25°C AND 50°C FOR CsF SOLUTIONS

Molal Conc.	25°C		25°C	
	$\delta_{\text{obs}}(\text{F}^{25}\text{-HFB}^{25})$ in ppm	$\delta_{\text{obs}}(\text{F}^{25}\text{-CFC}^{25})$ in ppm	$\Delta(\text{F}^{25}\text{-HFB}^{25})$ in ppm	$\Delta(\text{F}^{25}\text{-CFC}^{25})$ in ppm
0.74	-	2.716	-	-0.904
1.65	-50.006	-	-1.533	-
2.82	-	0.148	-	-1.087
4.38	-53.184	-	-1.988	-
6.64	-	-4.070	-	-1.940
9.15	-	-6.725	-	-2.090
11.78	-61.346	-9.716	-2.764	-2.516
17.81	-67.869	-	-3.184	-
26.50	-76.053	-	-3.618	-
	$\pm .024$	$\pm .020$	$\pm .041$	$\pm .030$

Molal Conc.	50°C	
	$\delta_{\text{obs}}(\text{F}^{50}\text{-HFB}^{50})$ in ppm	$\Delta(\text{F}^{50}\text{-HFB}^{50})$ in ppm
0.74	-48.214	-1.418
1.65	-49.546	-1.648
2.82	-51.001	-1.866
4.38	-52.962	-2.130
6.64	-55.687	-2.450
7.70	-56.901	-2.571
9.15	-58.495	-2.693
11.78	-61.456	-2.930
14.55	-64.940	-3.182
15.69	-65.697	-3.166
17.81	-67.761	-3.283
19.65	-69.416	-3.515
22.92	-72.497	-3.538
	$\pm .014$	$\pm .035$

TABLE VI: TABLE OF CHEMICAL SHIFTS AND BULK SUSCEPTIBILITIES
FOR AQUEOUS ALKALI METAL FLUORIDE SOLUTIONS

δ = Corrected Chemical Shift at Temperature Indicated
Relative to Para-difluorobenzene at 0°C in ppm

χ = Volume Magnetic Susceptibility in cgs - emu

Salt	Molality	0°C		25°C		50°C		100°C	
		$-\delta$	$-\chi \times 10^6$						
KF	0.17	1.899	0.763	-	-	-	-	-	-
	0.53	2.046	0.763	1.425	0.760	0.860	0.730	-0.874	0.719
	1.24	2.281	0.779	1.564	0.774	0.986	0.746	-0.811	0.722
	3.28	2.678	0.814	1.828	0.800	1.216	0.780	-0.736	0.743
	5.44	2.809	0.833	1.843	0.824	1.178	0.810	-1.034	0.786
	8.00	2.462	0.869	1.658	0.850	1.061	0.832	-1.119	0.805
	11.47	1.860	0.880	-	-	-	-	-1.813	0.845
	14.37	0.962	0.910	0.189	0.892	-0.304	0.871	-2.371	0.839
RbF	0.37	-	-	1.564	0.748	0.836	0.742	-	-
	0.78	2.447	0.762	1.781	0.763	-	-	-	-
	1.10	2.682	0.771	1.980	0.764	1.219	0.770	-	-
	1.69	2.939	0.780	2.147	0.778	1.465	0.772	-	-
	2.21	-	-	2.422	0.788	-	-	-	-
	2.78	3.411	0.804	2.631	0.803	1.909	0.795	-	-
	4.10	-	-	3.112	0.822	2.414	0.813	-	-
	4.40	3.966	0.833	-	-	-	-	-	-
	4.72	-	-	3.321	0.835	-	-	-	-
	5.38	4.283	0.848	3.528	0.846	2.939	0.814	-	-
	6.12	-	-	3.750	0.856	-	-	-	-
	6.52	4.657	0.857	-	-	3.320	0.826	-	-
	6.91	-	-	3.981	0.867	-	-	-	-
	7.50	-	-	4.152	0.864	3.596	0.839	-	-
	8.48	5.180	0.876	4.417	0.885	3.920	0.846	-	-
	9.96	-	-	4.837	0.897	4.353	0.866	-	-
11.72	5.992	0.921	5.316	0.914	4.867	0.885	-	-	
14.38	6.700	0.931	6.097	0.928	5.656	0.904	-	-	
CsF	0.74	-	-	2.573	0.750	2.019	0.739	-	-
	1.65	-	-	3.665	0.796	3.294	0.764	-	-
	2.82	-	-	5.084	0.777	4.684	0.797	-	-
	4.38	-	-	6.701	0.864	6.563	0.836	-	-
	6.64	-	-	9.034	0.905	9.188	0.884	-	-
	7.11	-	-	-	-	-	-	-	-
	7.70	-	-	-	-	10.364	0.902	-	-
	9.15	-	-	11.641	0.928	11.920	0.920	-	-
	9.87	-	-	-	-	-	-	-	-
	11.78	-	-	14.560	0.985	14.806	0.956	-	-
	12.65	-	-	-	-	-	-	-	-
	14.55	-	-	-	-	18.211	0.994	-	-
	15.69	-	-	-	-	18.974	0.991	-	-
	17.81	-	-	21.014	1.042	21.000	1.009	-	-
	19.65	-	-	-	-	22.582	1.044	-	-
	22.92	-	-	-	-	25.657	1.047	-	-
26.50	-	-	29.061	1.107	-	-	-	-	

DISCUSSION

For a given magnetic field strength the resonance frequency of a nucleus is dependent on its immediate electronic and nuclear environment. Small changes in this environment cause a resonance frequency shift. Thus, the study of chemical shifts of ions and water in aqueous electrolyte solutions as a function of concentration and temperature should yield a great deal of information about the structure of the solution.^{13,14,15}

Labile Equilibrium

In almost all aqueous solution studies and in this research, only one peak appears in the resonance spectra of the protons or ions. The resonance of frequency of this peak is a function of concentration and temperature. For protons (or ions) this occurs only if (a) all the protons (or ions) are in exactly the same state or (b) if the protons (or ions) are exchanging rapidly between several states while maintaining an equilibrium distribution among the states (labile equilibrium). It is unlikely that the protons (or ions) are all in the same state, because thermal motion of the molecules in solution causes the immediate environment of one nucleus to be different from another. One must, therefore, use a labile equilibrium approach to explain the resonance spectra of aqueous electrolyte solutions exhibiting only one peak.

The chemical shift of the single peak is then the average shift of the protons in the various states. This shift is related to the time average distribution function for the number of nuclei in each state:

$$\delta = \frac{1}{n} \sum_i n_i \delta_i \quad (11)$$

In equation (11) δ is the observed shift, δ_i is the chemical shift of state i , n_i is the number of nuclei in state i , and n is the total number of nuclei.

In particular, the fluoride ion exists in many different states. Each change in nuclear position relative to neighboring ions or water molecules constitutes a different state. The number of states is extremely large and, consequently, the chemical shift is very difficult to interpret in terms of the n_i and δ_i .

The labile equilibrium approach is made tractable by assuming that most of the states can be grouped into a few classes. Each class contains those states whose chemical shifts differ from the average chemical shift of the class by a small amount compared to the difference in average shifts between classes. The changes in shifts as a function of concentration and temperature are thus due to changes in the equilibrium distribution of ions among the classes. This simplified approach has been used with some degree of success to interpret the proton chemical shifts of aqueous electrolyte solutions.^{13,14,15,16,17}

How fast must the nuclei exchange between the several states for only one peak to appear in the spectrum? An order of magnitude estimate can be made by considering the condition for coalescence of two nmr peaks into one. If the chemical shift difference between the two peaks (classes), δ , is 2×10^{-6} and the frequency of the nmr spectrometer, ν_0 , is 56.4 MHz, then the residence time, τ , of a given nucleus in one of the classes must be less than that given by^{12,13}

$$2\pi \nu_0 \delta \tau \approx 1. \quad (12)$$

Thus, $\tau \leq 1.44 \times 10^{-4}$ seconds from the numbers given above.

Motivations for This Investigation

The next logical step in the labile equilibrium approach is to identify each class with a definite molecular species. For example, when explaining the chemical shift of the single peak appearing in the proton nmr spectrum of pure water as a function of temperature, one assumes that classes of states are identifiable respectively with water molecules having no hydrogen bonds, one hydrogen bond, two hydrogen bonds, etc. The relative numbers of these species comprise the equilibrium distribution.

Another way of treating the equilibrium distribution is to consider the classical equilibria between the assigned molecular species. One can then consider equilibrium constants in addition to the number of moles of each species.

In these terms the following questions concerning aqueous alkali metal fluoride solutions arise:

- 1) What are the species present in solution?
- 2) What are the relative numbers of each of these species, and how do these numbers change with concentration and temperature?
- 3) What equilibria are involved? What are the equilibrium constants?
- 4) What are the energetics of the reactions controlling the equilibria?
- 5) What are the chemical shifts of each of these species? Do these shifts change as a function of temperature?

The intention of this investigation is to attempt to answer these questions by measuring the F^{19} chemical shift of KF, RbF, and CsF as a function of concentration and temperature; and to explain the shifts using a labile equilibrium approach.

Trends of the Data

When considering the trends in the data, it is well to recall that positive chemical shifts are high field shifts, representing an increase in magnetic shielding. Downfield shifts are negative.

The chemical shift data, plotted in Figures 2 through 5, must be considered in terms of probable "species", because the single line that appears in the F^{19} spectrum of the fluoride ion in these solutions dictates the use of a labile equilibrium theory. All the curves are non-linear, the shifts moving downfield from the infinite dilution values with increasing concentration. For RbF and CsF , the F^{19} shifts continue downfield and become more linear as the concentration increases; however, for KF the F^{19} shift reaches a minimum and at high concentrations exhibits a more positive shift than at infinite dilution. The minimum is apparent at all temperatures. In order to explain the minimum within the framework of a labile equilibrium theory at least three species must be considered.

The aqueous salt species predominating in the dilute solutions will be designated the D-species. As the concentration increases an intermediate species (I-species) appears in increasing number. In more concentrated solutions a third structure, the C-species, is postulated.

Figure 5 shows that the infinite dilution chemical shifts are the same for all three salts. Other investigators of ion resonances in aqueous solutions have observed similar infinite dilutions intersections.^{18,19} Hence, the D-species must be the isolated aqueous (hydrated) fluoride ion. Isolation is complete enough at infinite dilution to negate cation effects. Furthermore, the dependence of the intersection on temperature represents the temperature dependence of the chemical shift of the isolated hydrated fluoride ion.

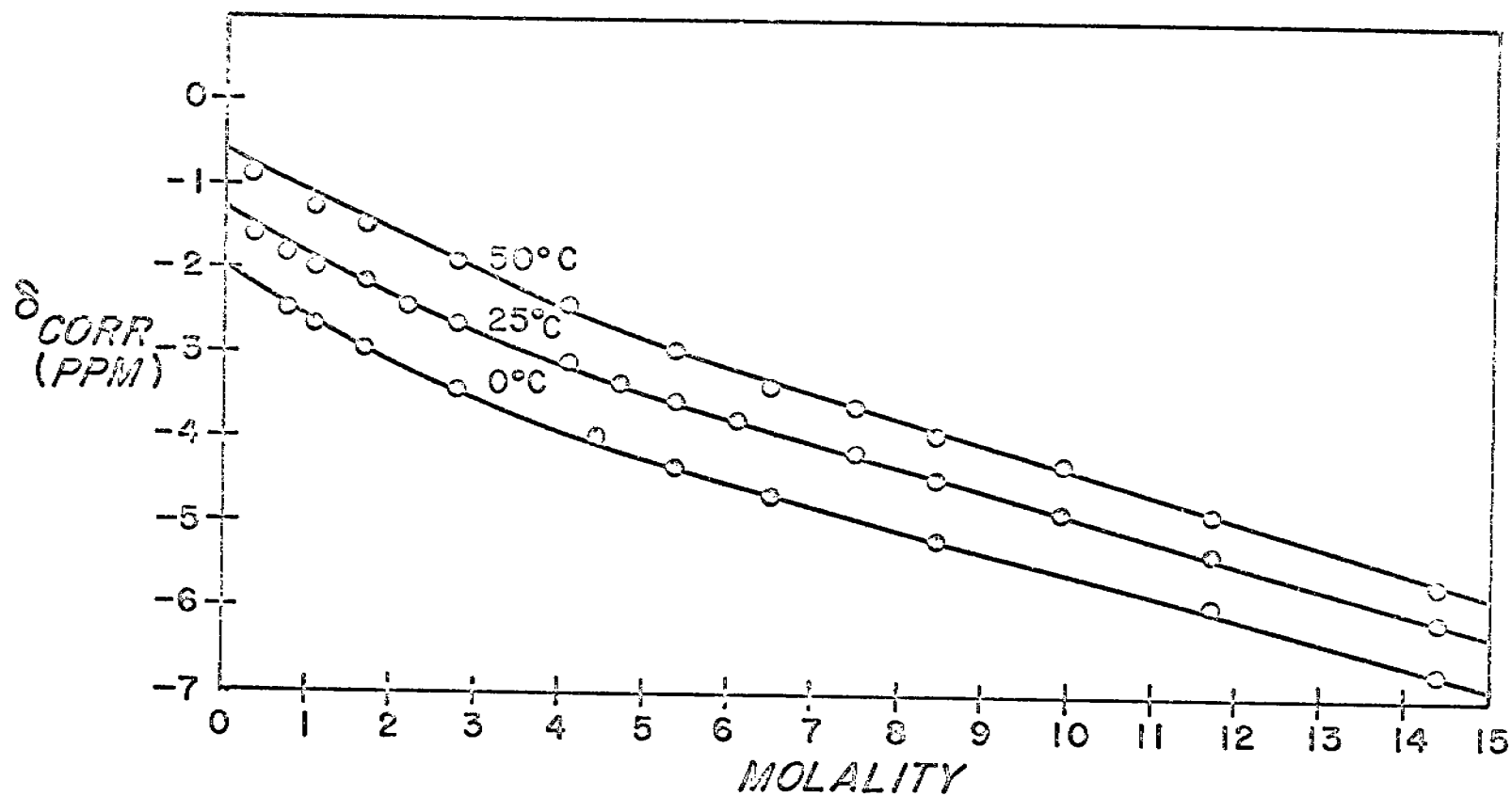


FIG. 2 F^{19} SHIFTS (RELATIVE TO P-DIFLUOROBENZENE AT 0°C) OF AQUEOUS RbF SOLUTIONS AS A FUNCTION OF MOLALITY AT DIFFERENT TEMPERATURES

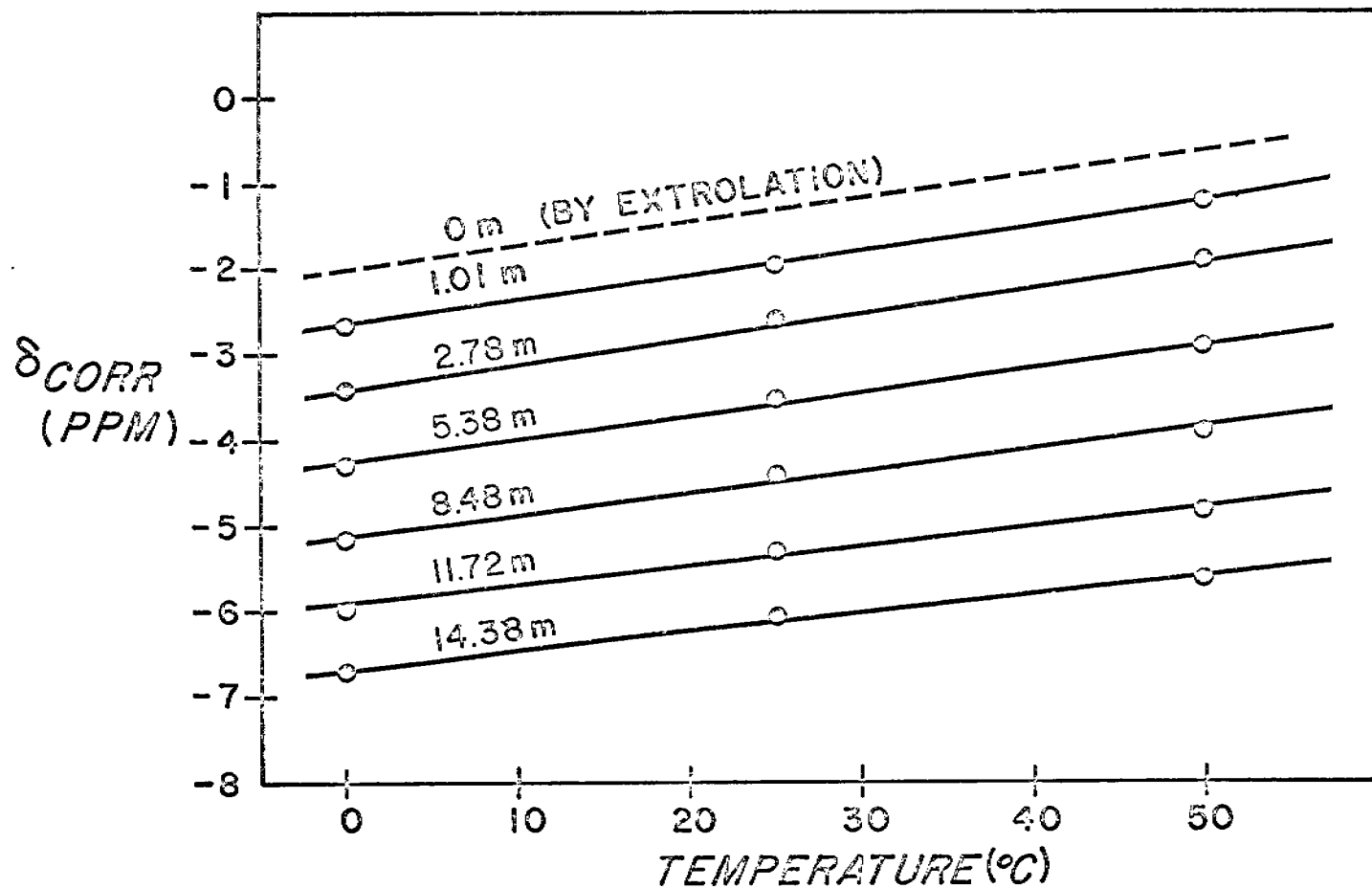


FIG. 3 F^{19} SHIFT (RELATIVE TO P-DIFLUOROBENZENE AT 0°C) OF AQUEOUS RbF SOLUTIONS AS A FUNCTION OF TEMPERATURE AT DIFFERENT MOLALITIES

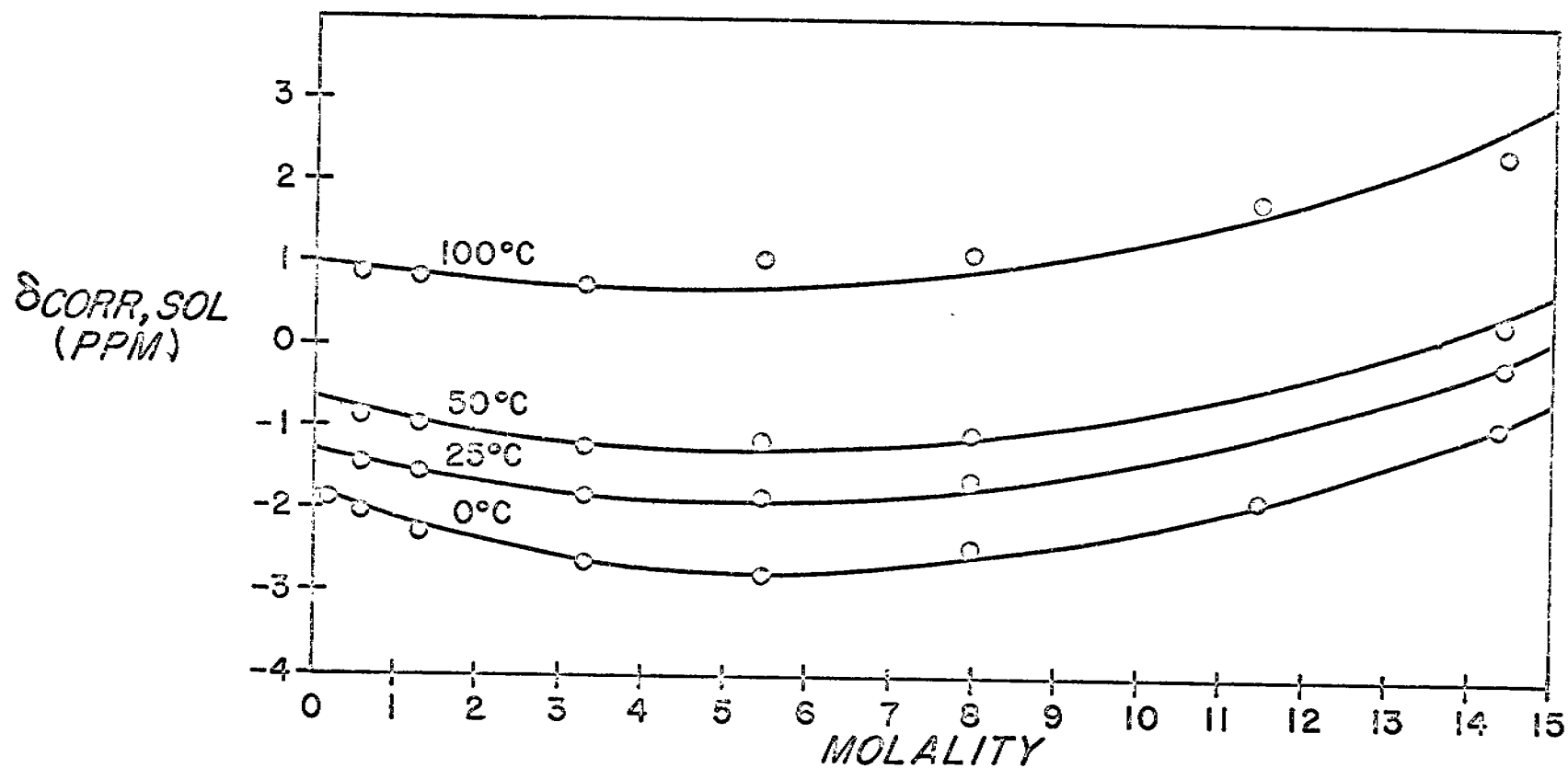


FIG. 4 ^{19}F SHIFT (RELATIVE TO P-DIFLUOROBENZENE AT 0°C) OF AQUEOUS KF SOLUTIONS AS A FUNCTION OF MOLALITY AT DIFFERENT TEMPERATURES

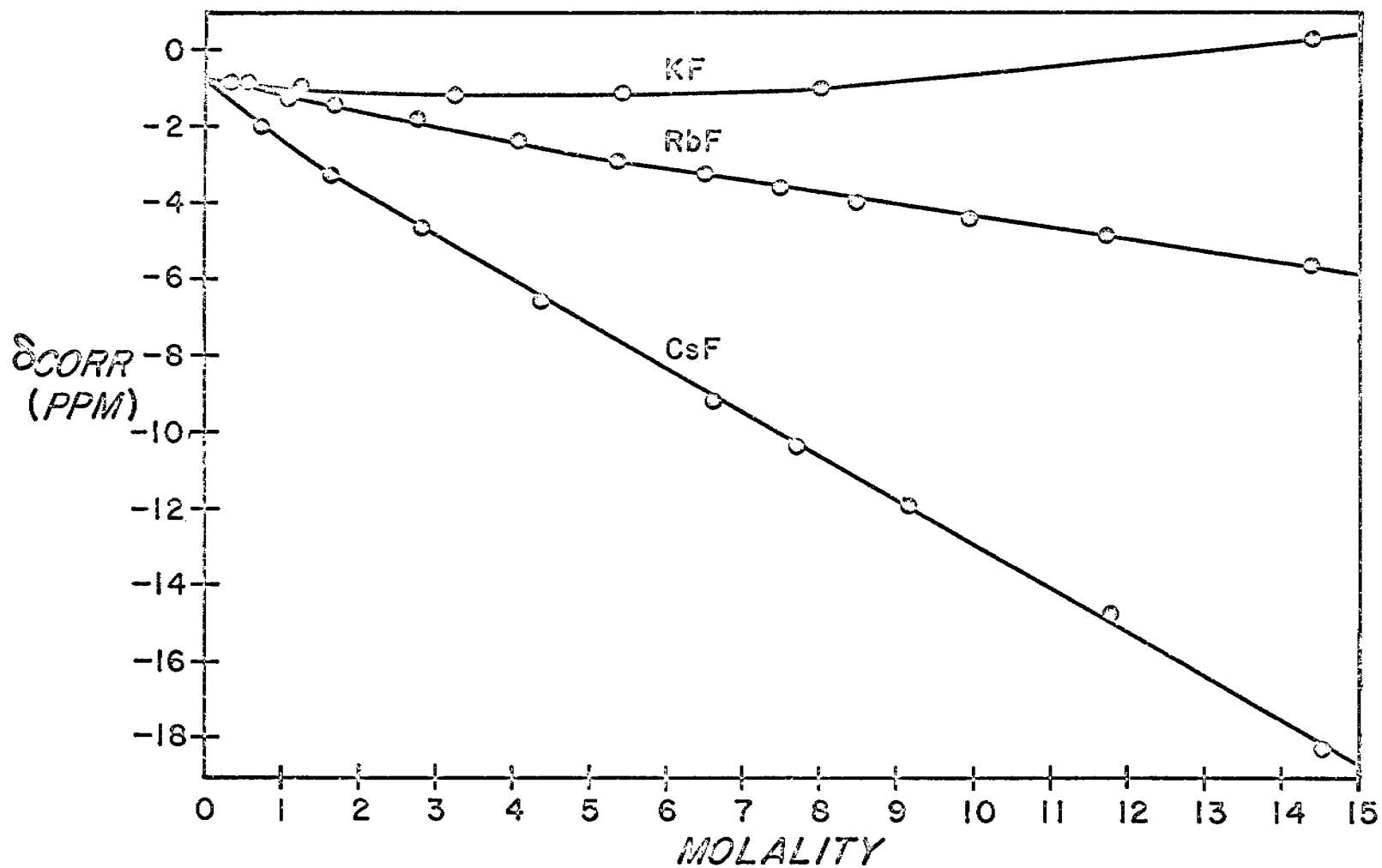


FIG. 5 F^{19} SHIFTS (RELATIVE TO P-DIFLUOROBENZENE AT 0°C) OF AQUEOUS KF, RbF AND CsF SOLUTIONS AS A FUNCTION OF MOLALITY AT 50°C

The downfield trend of the curves at low concentrations indicates that the I-species is less shielded than the D-species for all three salts observed. The minimum and recurve in the KF data imply that the C-species is more shielded than the D-species. The continuing downfield trends of the average chemical shift of the RbF and CsF solutions do not unequivocally allow us to determine the shift of the C-species. Most likely the C-species has a more positive shift than the I-species, but more negative than the D-species. It is highly unlikely that the alternative is true; namely, that the shift of the C-species is more positive than the D-species, but not present in sufficient number to cause the trend to turn upfield.

Notably, for any given salt, the same general shape of the shift-concentration curves persists at all temperatures. This is consistent with the labile equilibrium approach. Here, the chemical shifts of the individual species account for the gross displacements of the curves with temperature and the changes in the relative proportions of the individual species account for the slight changes in curvature. What is surprising is that the chemical shift is an approximately linear function of temperature at any given concentration; for example, see Figure 3.

As noted, there is no cation effect at infinite dilution. The magnitude of the negative shift of the observed signal increases thereafter in the order $K > Rb > Cs$, and the total range of the observed shift increases in the same order.

Curve Fitting

Inspection of the observed chemical shift data indicates a relatively simple dependence on molality; perhaps a second or third degree function. To determine this function more precisely the curves were analyzed by means of a polynomial least-squares scheme.

The best curve determined visually was drawn through the experimental points. Values of the chemical shift and molality were read from the curve at 1/2 molal intervals. These values were used as input for a polynomial least-squares scheme programmed for an IBM 360 computer.

Table VII lists values of the standard unbiased error calculated by computer for the polynomial of maximum degree indicated. The standard unbiased error, S , is given by

$$S = \pm \left[\frac{\sum_{i=1}^{(NP)} (\delta_i - \hat{\delta}_i)^2}{D} \right]^{1/2} \quad (13)$$

with

$$D = [(NP) - (MAXD)] + 1 \quad (14)$$

where NP is the number of points fitted with polynomial of maximum degree $MAXD$, δ_i is the measured value of the chemical shift at molality, m_i , and $\hat{\delta}_i$ is the chemical shift at m_i calculated using the polynomial for which S is being evaluated. For example, the standard unbiased error is 0.011 ppm for the polynomial of maximum degree 4 fitted to the chemical shift data of KF at 50°C.

The experimental error in the observed chemical shifts is ± 0.05 ppm for KF and RbF and ± 0.09 ppm for CsF. Thus a polynomial of at least second degree is necessary to fit the data within experimental error. At this point one is cautioned not to conclude that the experimental curves are truly second degree in nature. It is only evident that the accuracy of the observed chemical shift does not warrant using polynomials of higher degree.

TABLE VII: VALUES OF THE MEAN UNBIASED ERROR, S ,
TABULATED IN PPM

Fitted Data	----- Maximum Degree of Polynomial Used for the Fit -----						
	<u>0</u>	<u>1</u>	<u>2</u>	<u>3</u>	<u>4</u>	<u>5</u>	<u>6</u>
KF 0°C	0.550	0.460	0.190	0.180	0.180	0.180	0.180
25	0.510	0.330	0.025	0.005	0.005	0.005	0.004
50	0.530	0.280	0.021	0.010	0.011	0.009	0.010
100	0.540	0.240	0.020	0.008	0.002	0.003	0.004
RbF 0°C	1.340	0.170	0.078	0.019	0.012	0.012	0.010
25	1.390	0.110	0.049	0.016	0.009	0.010	0.013
50	1.480	0.130	0.047	0.008	0.008	0.004	0.005
CsF 25°C	6.280	0.140	0.120	0.078	0.046	0.030	0.108
50	6.580	0.240	0.140	0.086	0.055	0.030	0.110

To second degree then

$$\delta = a_0 + a_1 m + a_2 m^2 \quad (15)$$

The coefficients in equation (15) are listed in Table VIII.

TABLE VIII: COEFFICIENTS OF EQUATION (15)

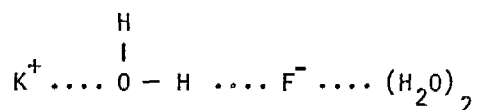
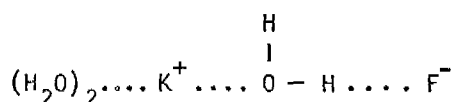
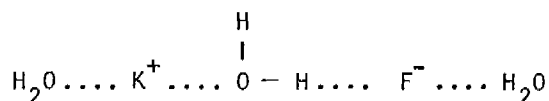
Fitted Data	a_0 (ppm)	a_1 $\left(\frac{\text{ppm}}{\text{mole}}\right)$	a_2 $\left(\frac{\text{ppm}}{[\text{mole}]^2}\right)$
KF 0°C	-1.843	-0.284	+0.024
25	-1.361	-0.191	+0.0193
50	-0.763	-0.126	+0.0158
100	+0.912	-0.090	+0.0138
RbF 0°C	-2.201	-0.434	+0.00904
25	-1.486	-0.402	+0.00599
50	-0.744	-0.434	+0.00678
CsF 25°C	-1.665	-1.132	+0.00300
50	-1.061	-1.261	+0.00756

The Physical Model

The physical model is discussed below with particular reference to potassium fluoride. Indeed, the chemical shift curve of KF is the most complicated of all the salts studied in this investigation. If the model proposed is successful in explaining the KF shift data, it is reasonable to expect that the same model, or a simpler modification thereof, should explain the RbF and CsF data.

In very dilute solutions there are extensive regions of normal water interspersed with ion sites. The ions are isolated from one another but solvated to water molecules. Estimates of the total hydration of the two ions (or of the hydration of the individual ions) vary widely¹⁴ because they depend on the experimental procedures involved, the definitions of hydration number used, the choice of the ion used to divide total hydration numbers into individual ion hydration numbers. A total hydration number of four was chosen for KF. This choice is justified below. The hydrated ions in this situation comprise the D-species.

For the I-species we postulate a potassium-water-fluoride aquo-ion pair. In the aquo-ion pair one water molecule is shared by both ions. Several possible structures exist:



Since the individual ion hydration numbers are not known it is difficult to decide which of these three structures is the I-species. In any case, the total hydration number is reduced to 3, whereas a total of four water-ion bonds still exists as in the D-species. The aquo-ion pair constitutes a convenient transition structure for the formation of the C-species from the D-species. The C-species, we postulate, consists of many potassium ions, fluoride ions, and water molecules mutually bonded with a ratio of two water molecules to one potassium-ion-fluoride-ion pair. It is

possible that four water-ion bonds per KF still exist. The time-average short-range order of this large "flickering" cluster probably resembles that of $\text{KF}\cdot 2\text{H}_2\text{O}$, the solid precipitating from concentrated solution at low temperatures. At all concentrations, dynamic equilibrium exists between the D- and I-species and between the I- and C-species.

Several factors influenced the structures postulated for the three species. Namely, the trends in the chemical shift data already noted; the shortage of water molecules in concentrated solutions; a theory²⁰ concerned with short-range order in aqueous electrolyte solutions; and the phase diagram for the potassium fluoride-water system.²¹ These points are discussed below.

A. Short-Range Order Theory

The postulate of the theory outlined in Samoilov's book²⁰ is that the short-range order in dilute solutions is primarily that of the solvent whereas the short-range order in concentrated solutions is primarily that of the salt precipitating from solution as the temperature is lowered. Also, at intermediate concentrations, there should be a transition structure bridging the gap between the two extreme short-range orders.

B. Phase Diagram

The short-range order theory implies that some aspects of the structure of the solution can be inferred from the structure of the solid phase that can exist in equilibrium with the solution. (Normally, such interpretation of the phase diagram is not sound because molecular rearrangements can occur during crystallization. An exception occurs when a congruent melting point appears in the phase diagram for the system).

C. Chemical Shift Data

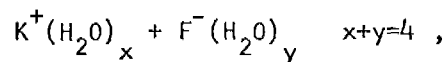
The formation of the aquo-ion pair readily explains why the chemical

shift curves do not approach the zero concentration chemical shift asymptotically. Namely, at the lowest concentration for which the ^{19}F line of the fluoride ion can be observed there are sufficient I-species present to influence the average shift. The observed shift would be independent of concentration in the dilute region if no aquo-ion pairs were present. Indeed, future experiments with improved instrumentation might reveal that the observed chemical shift is independent of concentration below 0.5 M. The presence of the I-species at low concentrations also explains the cation effect: viz, the deshielding of the fluoride ion within the aquo-ion pair should increase with increasing charge density on the cation. This would have the effect of increasing the range of the total shifts and of the initial downfield shifts in the order $\text{Cs}^+ > \text{Rb}^+ > \text{K}^+$.

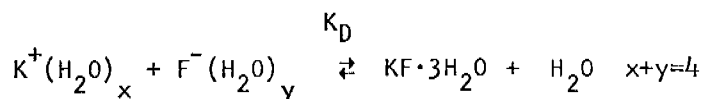
The structure of crystalline $\text{KF}\cdot 2\text{H}_2\text{O}$ is orthorhombic.²³ If this highly symmetrical structure persists in solution as the C-species, it is expected that the fluoride ion in this situation would be more shielded than the fluoride ion in the D-species. Hence, the C-species would have a more positive shift than the D-species as required by the minimum in the KF curve.

Mathematical Development

The three species proposed exist in mutual equilibrium. In light of the previous discussion the D-species can be represented by

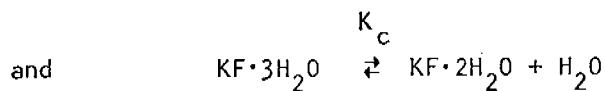


the I-species by $\text{KF}\cdot 3\text{H}_2\text{O}$, and the C-species by $\text{KF}\cdot 2\text{H}_2\text{O}$. The equilibria between these species are:



with

$$K_D = \frac{m_I m_w}{m_D} \quad (16)$$



with

$$K_C = \frac{m_C m_w}{m_I} \quad (17)$$

The chemical symbols m_w , m_I , m_D and m_C appearing in equations (16) and (17) are the equilibrium molalities of free (unbound) water, species I, D and C, respectively. Throughout this development the words molality and moles will be used interchangeably. Thus, it is to be understood that moles means the number of moles per 55.50 moles of water. There are two restrictions on the molalities in equations (16) and (17), namely,

$$m = m_D + m_I + m_C \quad (18)$$

and

$$m_w = a - 4m_D - 3m_I - 2m_C, \quad (19)$$

where $a = 55.50$, the number of moles in 1000 gm of water, and m is the stoichiometric molality of KF.

In these terms the average chemical shift of the fluoride ion is

$$\delta = \frac{m_D}{m} \delta_D + \frac{m_I}{m} \delta_I + \frac{m_C}{m} \delta_C \quad (20)$$

or, after substitution of equation (8),

$$\delta = \delta_D + \frac{m_I}{m} (\delta_I - \delta_D) + \frac{m_C}{m} (\delta_C - \delta_D) \quad (21)$$

To relate equation (21) to the experimental shift data, equations (16) through (19) must be solved for $\frac{m_I}{m}$ and $\frac{m_C}{m}$ as a function of m . To proceed, equations (18) and (19) are substituted in equations (16) and (17), yielding

$$K_D = \frac{m_I (a - 4m + m_I + 2m_C)}{(m - m_I - m_C)^2} \quad (22)$$

$$K_C = \frac{m_C (a - 4m + m_I + 2m_C)}{m_I} \quad (23)$$

These two coupled equations cannot be solved for $\frac{m_I}{m}$ and $\frac{m_C}{m}$ in closed form. However, a double iteration technique yields uncoupled solutions for $\frac{m_I}{m}$ and $\frac{m_C}{m}$ as a function of m that is valid at low concentrations.

First, equations (22) and (23) must be rearranged and expanded in terms of m , m_I , and m_C .

Thus, from equation (22)

$$\begin{aligned} \frac{m_I}{m} &= \frac{K_D}{a} \frac{\frac{1}{m}(m - m_I - m_C)^2}{1 + \frac{m_I - 4m + 2m_C}{a}} \\ &= \frac{K_D}{am} (m - m_I - m_C)^2 (1 - \alpha + \alpha^2 - \dots) \end{aligned} \quad (24)$$

and from equation (23)

$$\begin{aligned} \frac{m_c}{m} &= \frac{m_l}{m} \left[\frac{K_c}{a} \frac{1}{1 + \frac{m_l - 4m + 2m_c}{a}} \right] \\ &= \frac{m_l}{m} \left[\frac{K_c}{a} (1 - \alpha + \alpha^2 - \dots) \right]. \end{aligned} \quad (25)$$

In both equations $\alpha = \frac{1}{a} (m_l - 4m + 2m_c)$. The expansion converges for all concentrations of interest, because α is less than unity for these concentrations. The approximation for the dilute region consists of neglecting terms of order higher than zero, one, and two in succession; and, at each step, determining an uncoupled solution that is valid to the order of approximation.

To zero order in the molalities the results are

$$\frac{m_l}{m} = 0 \quad \text{and} \quad \frac{m_c}{m} = 0$$

Keeping terms to first order in the molalities we find

$$\frac{m_l}{m} = \frac{K_D}{a} (m - 2m_l - 2m_c + 2m_l \frac{m_c}{m} + m_l \frac{m_l}{m} + m_c \frac{m_c}{m}) \quad (26)$$

and

$$\frac{m_c}{m} = \frac{m_l}{m} \frac{K_c}{a} \left(1 - \frac{m_l - 4m + 2m_c}{a} \right). \quad (27)$$

Substituting the zero order approximation for $\frac{m_l}{m}$ and $\frac{m_c}{m}$ into equations (26) and (27) we find

$$\frac{m_c}{m} = 0 \quad \text{and} \quad \frac{m_l}{m} = \frac{K_D}{a} m .$$

Substitution of these values back into equations (26) and (27) completes the iteration process for the first-order solutions, yielding

$$\frac{m_c}{m} = \frac{K_D K_C}{a^2} m \quad \text{and} \quad \frac{m_l}{m} = \frac{K_D}{a} m . \quad (28)$$

Further iteration only produces the solutions expressed in these equations.

Solutions that are valid to second order in molality are obtained by keeping terms to second order throughout the entire approximate iteration scheme. These solutions are:

$$\frac{m_l}{m} = m \frac{K_D}{a} \left[1 - m \left\{ \frac{2K_D}{a} \left(1 + \frac{K_C}{a} \right) - \frac{4}{a} \right\} \right] \quad (29)$$

and

$$\frac{m_c}{m} = m \frac{K_D K_C}{a^2} \left[1 - m \left\{ \frac{2K_D}{a} \left(1 + \frac{K_C}{a} \right) - \frac{8}{a} \right\} \right] \quad (30)$$

The accuracy of the experimental data does not warrant extending the approximation to higher orders. It should be recalled, that a curve fitted polynomial of second degree reproduces the data satisfactorily.

An equation for the theoretical chemical shift as a function of molality that is valid to second order results from the substitution of equations (29) and (30) into equation (21); namely,

$$\delta = a_0 + a_1 m + a_2 m^2$$

where

$$a_0 = \delta_D \quad (31)$$

$$a_1 = \frac{K_D}{a} (\delta_I - \delta_D) + \frac{K_D K_C}{a^2} (\delta_C - \delta_D) \quad (32)$$

and

$$a_2 = \frac{K_D}{a} \left[\frac{2K_D}{a} \left(1 + \frac{K_C}{a} \right) - \frac{4}{a} \right] (\delta_D - \delta_I) \\ + \frac{K_D K_C}{a^2} \left[\frac{2K_D}{a} \left(1 + \frac{K_C}{a} \right) + \frac{8}{a} \right] (\delta_D - \delta_C) . \quad (33)$$

There are five parameters (δ_D , δ_I , δ_C , K_D , and K_C) in these equations and only three experimental coefficients (obtained from curve fitting). The parameter δ_D can be calculated without ambiguity. In the dilute region, one expects m_C to be small compared to m_I and so small compared to m_D that it can be neglected entirely. This is expressed in equations (31) through (33) by setting $K_C \cong 0$. The equation for the theoretical chemical shift is then,

$$\delta = \delta_D + \left[\frac{K_D}{a} (\delta_I - \delta_D) \right] \left[m + \left\{ \frac{2}{a} (2 - K_D) \right\} m^2 \right] . \quad (34)$$

From this equation the parameters related to the dilute and intermediate species can be calculated from the experimental data.

In retrospect, equation (34) is valid for low concentrations only. Effectively, the model has been reduced to a two state theory. As stated earlier, a two state model cannot predict an extremum in the chemical shifts as a function of concentration.

Correlation of Theory with Experiment

Comparison of the coefficients of the molality terms in equation (34) with the curve-fitted coefficients allows calculation of K_D , δ_1 , and δ_D . For example, from Table VIII, $a_0 = -1.361$, $a_1 = -0.191$, and $a_2 = +0.0193$ for KF at 25°C. Since

$$\frac{a_2}{a_1} = \frac{2}{a} (2 - K_D) , \quad (35)$$

$$a_1 = \frac{K_D}{a} (\delta_1 - \delta_D) , \quad (36)$$

and

$$a_0 = \delta_D . \quad (37)$$

we find, $\delta_D = -1.361$ ppm, $\delta_1 = -3.57$ ppm, and $K_D = 4.8$. Table VIII presents the coefficients of fitted second degree polynomials for the three salts studied. The values of δ_D , δ_1 , and K_D , calculated from these coefficients at various temperatures, appear in Table IX.

Equation (34) must be changed slightly if it is to apply to RbF and CsF. That is, for CsF solutions, the hydration number of the D-species is three (chosen to correspond with the phase diagram²⁴). In place of equation (34)

$$\delta = \delta_D + \left[\frac{K_D}{a} (\delta_1 - \delta_D) \right] \left[m + \left\{ \frac{1}{a} (3 - 2K_D) \right\} m^2 \right] ; \quad (38)$$

and in place of equation (35)

$$\frac{a_2}{a_1} = \frac{1}{a} (3 - 2K_D) . \quad (39)$$

TABLE IX: THE PARAMETERS OF THE LABILE EQUILIBRIUM THEORY AS CALCULATED WITH EQS. 35-39

Salt	Temp. ($^{\circ}\text{C}$)	K_D	δ_D (ppm)	δ_1 (ppm)
Hydration of D species = 4				
KF	0	4.38	-1.843	- 5.44
	25	$4.82 \pm .07$	$-1.361 \pm .052$	$- 3.57 \pm 0.20$
	50	5.48	-0.703	- 1.98
	100	6.26	+0.912	+ 0.11
Hydration of D species = 4				
RbF	0	2.58	-2.201	-11.55
	25	$2.41 \pm .05$	$-1.486 \pm .030$	-10.74 ± 0.20
	50	2.43	-0.744	-10.02
Hydration of D species = 3				
RbF	0	2.08	-2.201	-13.90
	25	1.91 ± 0.02	$-1.486 \pm .030$	-13.16 ± 0.10
	50	1.93	-0.744	-13.21
Hydration of D species = 3				
CsF	25	$1.57 \pm .20$	$-1.665 \pm .110$	-41.66 ± 2.0
	50	1.67	-1.061	-42.96

Inspection of the phase diagram of RbF^{25} reveals that the hydration number of the D-species can be either three or four; for which either equation (34) and (35) or equations (38) and (39) apply, respectively. Values of the parameters calculated for both possible hydration numbers are given in the Table IX. Errors are estimated at 25°C .

Range of Validity of the Dilute Approximation

An upper concentration limit for the validity of the dilute solution approximation of the theoretical chemical shift can be estimated by extending equation (29) for $\frac{m_1}{m}$. That is, with $K_C \cong 0$, the iteration process involving only equation 14 is easily carried to third order. The result is

$$\frac{m_1}{m} = \frac{K_D m}{a} \left[1 + \frac{2m}{a} (2 - K_D) - \frac{m^2}{a^2} (3K_D^2 + K_D - 16) \right] \quad (40)$$

For potassium fluoride at 25°C the third term inside the brackets of equation (40) is approximately 24% and 10% of the sum of the first two terms at $3m$ and $2m$, respectively. Thus it is expected that calculated values of $\frac{m_1}{m}$ are reliable within 25% at 3 molal. The reliability is probably better than 25%, because the higher order terms that were neglected in arriving at equation (40) have a cancelling effect on the last term inside the brackets. Of course, this estimate does not take into account any errors introduced by setting $K_C \cong 0$.

Verification of the Theory

The experimental data and the theory (both the physical model and mathematical structure) are internally consistent. Using the theory one can successfully explain the qualitative features of the chemical shift curves within the estimated region of validity (i.e., below 3 molal). Further independent verifications of the theory are necessary. First, the

results of this work will be applied to predict partial molar heat content of KF, which will be compared to experimental results. Secondly, K_D for KF will be calculated from ^{39}K nmr shifts.

A. Partial Molar Heat Content

Table IX contains values of the equilibrium constants K_D as a function of temperature. In Figure 6 the natural logarithm of K_D is plotted against $1/T$ for each salt. The slopes of such plots are related to the heat of the labile equilibrium reaction, ΔH_D . That is, the slope equals $-\Delta H_D/R$. For KF, we find $\Delta H_D = 706$ cal/mole. For RbF the errors are large and we find ΔH_D to be somewhere between 0 to -400 cal/mole when the hydration number of the D-species is 4. In the case of CsF the errors are too large for estimating ΔH_D .

These heats of reaction are related to the changes in the partial molar heat content of the solute in binary aqueous metal fluoride solutions. The total heat content of such a solution can be written as

$$H = n_1 \bar{H}_1 + n_2 \bar{H}_2, \quad (41)$$

where \bar{H}_1 and \bar{H}_2 , both functions of n_1 and n_2 , are the partial molar heat content of the solvent and solute respectively. The n 's are the number of moles of each substance. Within the framework of the dilute solution approximation, the solute is composed of the D- and I-species. For a solution composed of m moles of solute and 55.5 moles of water,

$$m \bar{H}_2 = (m - m_1) H_D + m_1 H_I. \quad (42)$$

or

$$\bar{H}_2 = H_D + \frac{m_1}{m} (H_I - H_D), \quad (43)$$

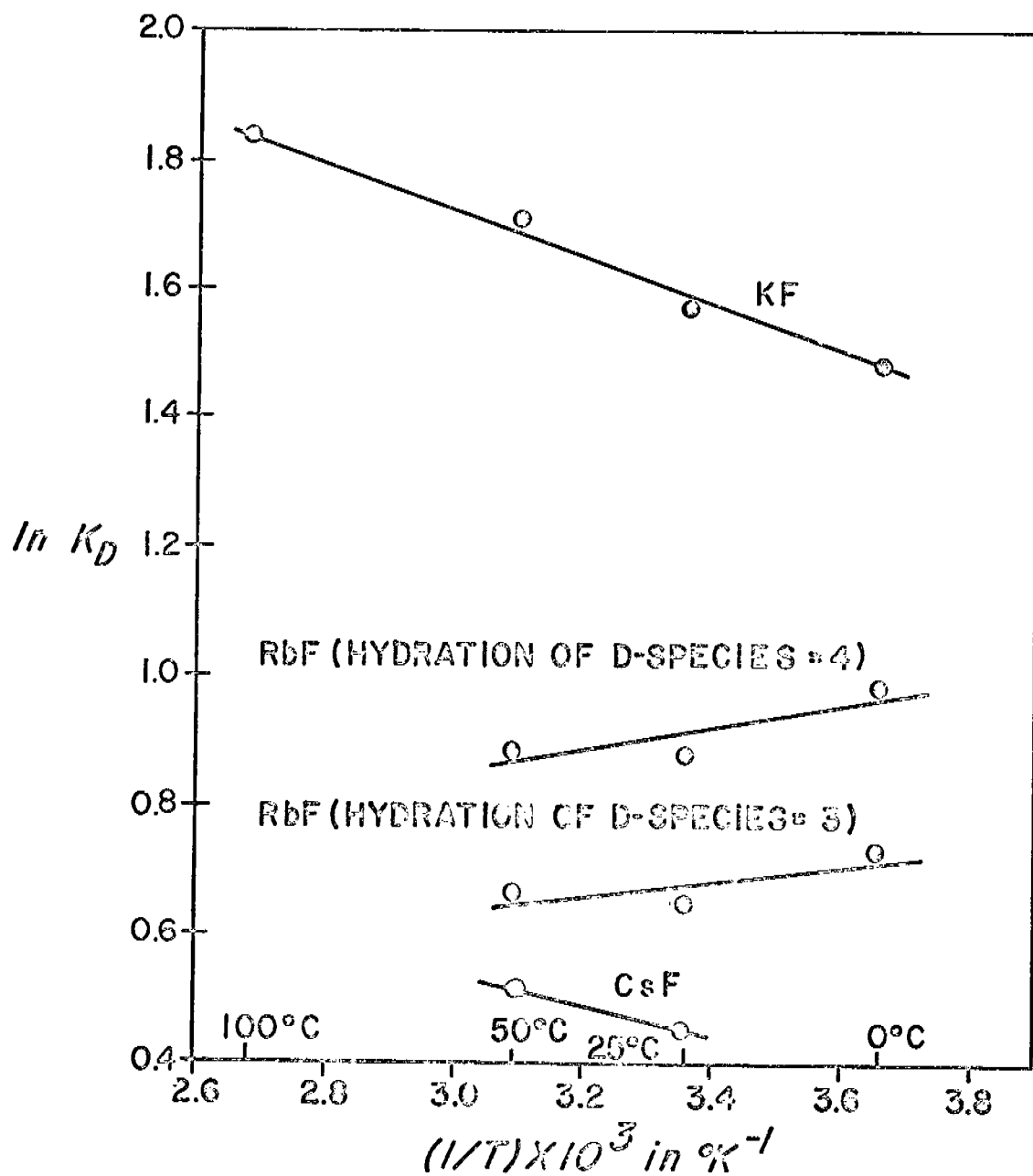


FIG. 6 NATURAL LOGARITHM OF THE EQUILIBRIUM CONSTANT K_D AS A FUNCTION OF $1/T$. DATA TAKEN FROM TABLE IX.

where H_I and H_D are independent of molality.

Thus the change in partial molar heat content of the solute for a change in concentration Δm is

$$\Delta \bar{H}_2 = \left(\Delta \frac{m_1}{m} \right) (\Delta H_D) \quad (44)$$

where $\Delta H_D = (H_I - H_D)$. In the second column of Table X values of $\frac{m_1}{m}$ are listed. These values are calculated using equation (29) after setting $K_C = 0$, and $K_D = 4.8$ as found for KF at 25°C. In column 3 the values of $\frac{m_1}{m}$, listed in column 2, are multiplied by ΔH_D for KF, 706 cal/mole. The fourth column contains the differences, $\left(\Delta \frac{m_1}{m} \right) (\Delta H_D)$ between successive values of the third column. The partial molar heat content, \bar{H}_2 , as given by Harned and Owen²⁶ are listed in column 5. Values for $\Delta \bar{H}_2$, shown in column 6, are gotten by taking differences between successive values of the fifth column. By comparing columns 4 and 6 it is clear that the theory adequately predicts changes in the partial molar heat content of KF over the concentration range which the theory is expected to be valid. Data for the partial molar heat content of RbF and CsF is not available for comparison. Indeed, even if such data were available, the estimates of ΔH_D are too crude for these compounds to allow meaningful comparison.

B. Potassium Resonance Data

Deverell and Richards¹⁹ have measured the cation resonance in several different alkali metal halide solutions at 25°C including potassium fluoride, but not cesium or rubidium fluoride. Their chemical shift data, measured by varying the frequency of the nmr spectrometer at a fixed magnetic field of 12,500 gauss, were published in graphical form. The shifts were uncorrected for bulk magnetic susceptibility effects. Before using this data we first

TABLE X: COMPARISON OF CALCULATED CHANGES IN THE PARTIAL MOLAR HEAT
 CONTENT OF KF AT 25°C WITH THOSE GIVEN BY HARNED AND OWEN²⁶

Molality KF	$\frac{m_1}{m}$	$\frac{m_1}{m} \Delta H_D \frac{\text{cal}}{\text{mol}}$	$(\Delta \frac{m_1}{m}) (\Delta H_D) \frac{\text{cal}}{\text{mol}}$	$\bar{H}_2 (15) \frac{\text{cal}}{\text{mol}}$	$\Delta \bar{H}_2 \frac{\text{cal}}{\text{mol}}$
0.1	0.0086	6.1		155	
0.2	0.0170	12.0	5.9	179	24
0.3	0.0252	17.8	5.8	190	11
0.4	0.0333	23.5	5.7	197	7
0.5	0.0411	29.0	5.5	203	6
0.6	0.0488	34.5	5.5	209	6
0.7	0.0564	39.8	5.3	215	6
0.8	0.0637	45.0	5.2	220	5
0.9	0.0709	50.1	5.1	226	6
1.0	0.0779	55.0	4.9	231	5
1.2	0.0913	64.5	9.5	240	9
1.5	0.1101	77.7	13.7	254	14
1.7	0.1219	86.1	8.4	262	8
2.0	0.1381	97.5	11.4	274	12
2.5	0.1616	114.1	16.6	291	17
3.0	0.1807	127.6	13.5	318	27
3.5	0.1953	137.9	10.3	376	58
4.0	0.2056	145.2	7.3	456	80
4.5	0.2114	149.2	4.0	546	90
5.0	0.2128	150.2	3.0	643	97
5.5	0.2098	148.1	-2.1	754	111
6.0	0.2025	143.0	-5.1	884	130

changed the sign of the shifts since a shift to higher frequency corresponds to a decrease in shielding when a fixed field-variable frequency technique is used. We then curve fitted to second degree the ^{39}K chemical shift of KF solutions. A value of $K_D = 2.5$ was obtained from the coefficients of the curve fitting. Agreement with K_D calculated from the ^{19}F shifts, 4.8, is quite good considering the relative crudeness of the graphical data of Deverell and Richards.¹⁹

CONCLUSIONS

It is apparent that the physical model proposed and the mathematical theory based thereon adequately explains the observed chemical shifts for dilute and moderately concentrated solutions. A mathematical solution could not be developed when the concentrated solution species was included.

For KF solutions, the agreement between published heat data and predicted heat changes is remarkable. Further verification of the theory is afforded by the good agreement between the values of K_D calculated from data obtained in this research and the potassium resonance shifts of Deverell and Richards,¹⁹ viz. 4.8 and 2.5, respectively. The uncertain values of the heat of reaction calculated for rubidium and cesium fluoride and the lack of compatible data involving the physical properties of aqueous solutions of these salts do not allow further verification of the model.

SUGGESTIONS FOR FUTURE WORK

The remarkable success of the theory as applied to potassium fluoride solutions provides a guide to future experimentation. Many compounds are likely choices for such experiments, but preference is given to those that form stable crystalline hydrates (in order to allow one to determine the short-range order in the C-species). These electrolytes should have a nucleus with non-zero spin.

The extensive work of Carrington¹⁸ et. al. concerning the chemical shift of the fluoride ion in mixed solvents can be extended to elevated temperatures. These experiments should yield information concerning the nature of the hydration of the D- and I-species. Experiments involving cation, anion effects, and mixed salt effects should yield information about the aquo-ion pair that comprises the I-species. Many experiments of this type have already been performed,^{18,19} but are incomplete and not suited for interpretation in the light of the theory developed herein.

Furthermore, with all of the experiments mentioned, the proton chemical shift of the solutions concerned should be measured concurrently. It has recently been shown^{15,27} that hydration numbers in dilute solutions can be determined from such data. In fact, the proton chemical shifts in KF solutions confirm the choice of 4 and 3 for the total hydration numbers of the D- and I-species, respectively.

REFERENCES

1. G. A. Williams and H. S. Gutowsky, *J. Chem. Phys.*, 25, 1288 (1956).
2. J. R. Zimmerman and M. R. Foster, *J. Phys. Chem.*, 61, 282 (1957).
3. M. G. Morin, G. Paulett and M. E. Hobbs, *J. Phys. Chem.*, 60, 1594 (1956).
4. Wilmad Glass Co., Buena, N. J., 08310. Part Numbers 516-1 (5 mm) and 516-0 (5 mm).
5. R. F. Spanier, T. Vladimiroff and E. R. Malinowski, *J. Chem. Phys.*, 45, 4355 (1966).
6. For example, H. S. Gutowsky, Geneva G. Bedford, and R. E. McMahon, *J. Chem. Phys.*, 36(12), 3353 (1962).
7. L. Petrakis and C. H. Sederholm, *J. Chem. Phys.*, 35, 1174 (1961).
8. An analogous equation has been derived by E. G. Paul and D. M. Grant, *J. Am. Chem. Soc.*, 86, 2977 (1964).
9. J. D. Baldeschweiler, *J. Chem. Phys.*, 36, 152 (1962).
10. L. G. Alexakos and C. D. Cornwell, *Rev. Sci. Inst.* 34, 790 (1963).
11. P. W. Anagan and C. E. Godsey, private communication.
12. J. A. Pople, W. G. Schneider, and H. J. Bernstein, High Resolution Nuclear Magnetic Resonance, McGraw-Hill Book Co., Inc., New York, 1959.
13. H. G. Hertz, *Ber. Bunseng. für Physikalische Chemie*, 67 (3), 311 (1963), and references therein.
14. J. F. Hinton and E. S. Amis, *Chemical Reviews*, 67 (4), 367 (1967), and references therein.
15. E. R. Malinowski, P. S. Knapp, B. Feuer, *J. Chem. Phys.*, 45 (11), 4274 (1966); 47 (1), 347 (1967).

16. J. C. Hindman, *J. Chem. Phys.*, 36 (4), 1000 (1962).
17. J. N. Shoolery, B. J. Alder, *J. Chem. Phys.*, 23 (5), 805 (1955).
18. A. Carrington, F. Dravnick, and M.C.H. Symons, *Mol. Phys.*, 3, 174 (1960).
19. C. Deverell and R. E. Richards, *Mol. Phys.*, 10, 551 (1966).
20. O. Ya Samoilov, Structure of Aqueous Electrolyte Solutions and the Hydration of Ions. Consultants Bureau, New York, 1965.
21. J. W. Mellor, A Comprehensive Treatise on Inorganic and Theoretical Chemistry, Volume II, Supplement III, John Wiley & Sons, New York, 1963, p. 1658.
22. E. R. Malinowski and A. Anton, private communication.
23. T. H. Anderson and E. C. Lingafelter, *Acta Cryst.* 4, 181 (1951).
24. Roger Cohen-Adad and Claude Ferlin, *Comptes rendus*, 258, 4057 (1964).
25. Roger Cohen-Adad and Claude Ferlin, *Comptes rendus*, 257, 2287 (1963).
26. H. S. Harned and B. B. Owen, The Physical Chemistry of Electrolytic Solutions, 3d Edition, Reinhold Publishing Corp., New York 1958.
27. R. E. Schuster and A. Fratiello, *J. Chem. Phys.*, 47, 1554 (1967).
28. V. B. Parker, "Thermal Properties of Uni-Univalent Electrolytes," National Standard Reference Data Series, National Bureau of Standards 2, (1965).

RESEARCH PERSONNEL

1. Dr. E. R. Malinowski, Principal Investigator
2. Mr. R. F. Spanier, Research Assistant
3. Mr. P. H. Weiner, Research Assistant
4. Mr. P. Dibello, Research Assistant
5. Mr. P. Knapp, Research Assistant

DEGREES ATTAINED OR EXPECTED

1. R. F. Spanier (to defend Ph.D. thesis in January, 1968).
2. P. Knapp (to defend Ph.D. thesis in January, 1968).
3. P. H. Weiner (obtained M.S. in June, 1966).
4. P. Dibello (obtained M.S. in June, 1966).

LIST OF PUBLICATIONS

1. Bulk Magnetic Susceptibilities Determined from NMR Spinning Sidebands Using Coaxial Cells, R. F. Spanier, T. Vladimiroff and E. R. Malinowski, J. Chem. Phys., 45, 4355 (1966).
2. Reference Standard for Studies Involving Temperature Dependence of F^{19} Chemical Shifts, R. F. Spanier and E. R. Malinowski, J. Chem. Phys., 47 (4), 1560 (1967).

PAPERS TO BE SUBMITTED FOR PUBLICATION

1. Temperature-Dependent Shift of Fluoride Ion at Infinite Dilution in Aqueous Solutions.
2. Temperature-Dependent Shift of F^{19} in Aqueous Solutions of KF, RbF and CsF.